Enhanced pseudocapacitive energy storage and thermal stability of Sn^{+2} ion-intercalated molybdenum titanium carbide (Mo_2TiC_2) MXene

Irfan Ali, Zulqarnain Haider, Syed Rizwan*

[a] Physics Characterization and Simulations Lab (PCSL), Department of Physics, School of Natural Sciences (SNS), National University of Sciences and Technology (NUST), Islamabad 44000, Pakistan.

Supplementary Information

SEM Data:

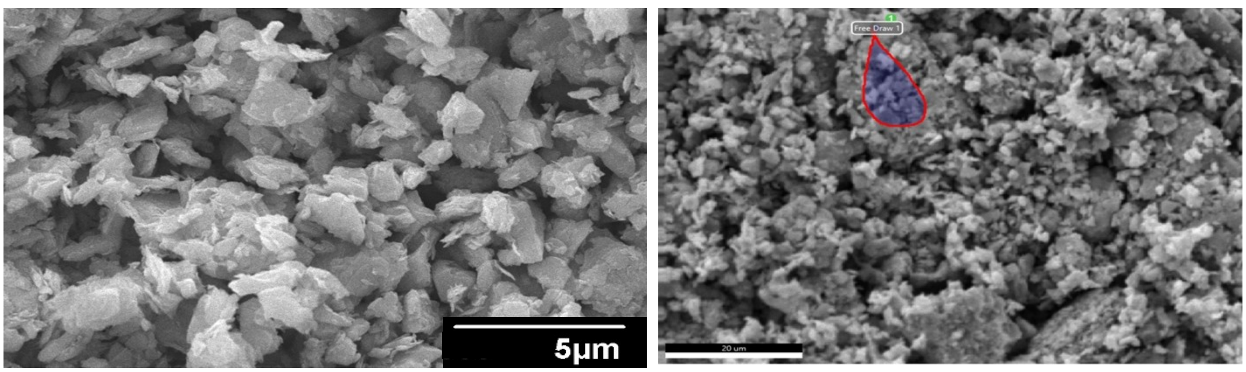

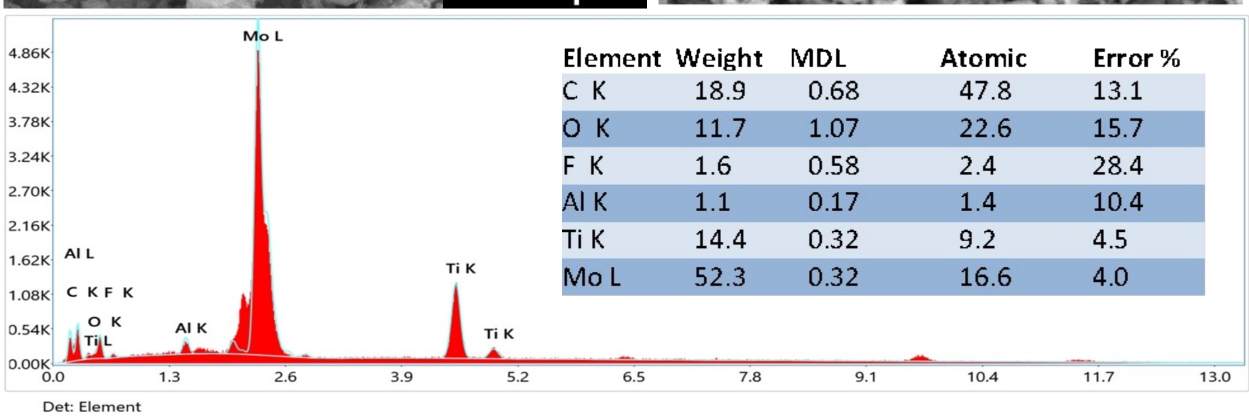

Element	Weight	MDL	Atomic	Error %
C K	18.9	0.68	47.8	13.1
O K	11.7	1.07	22.6	15.7
F K	1.6	0.58	2.4	28.4
Al K	1.1	0.17	1.4	10.4
Ti K	14.4	0.32	9.2	4.5
Mo L	52.3	0.32	16.6	4.0

Figure 1: Mo_2TiC_2 MXene SEM image along with their EDX data.

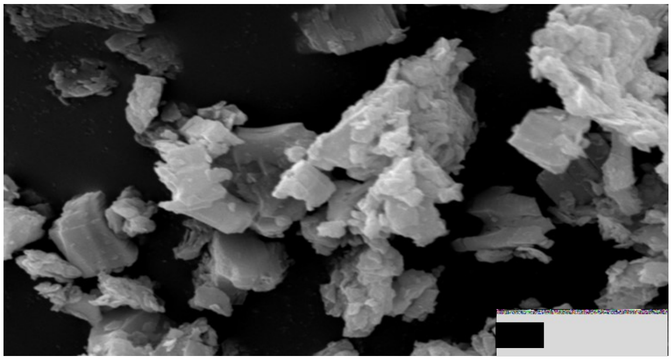

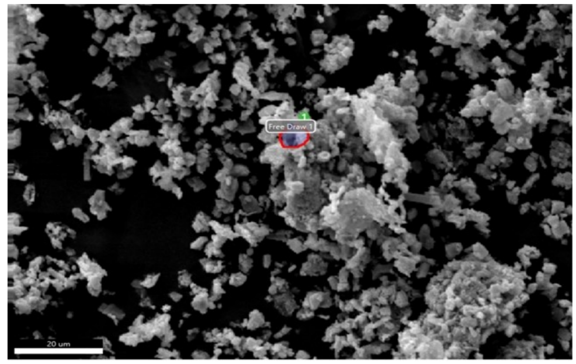

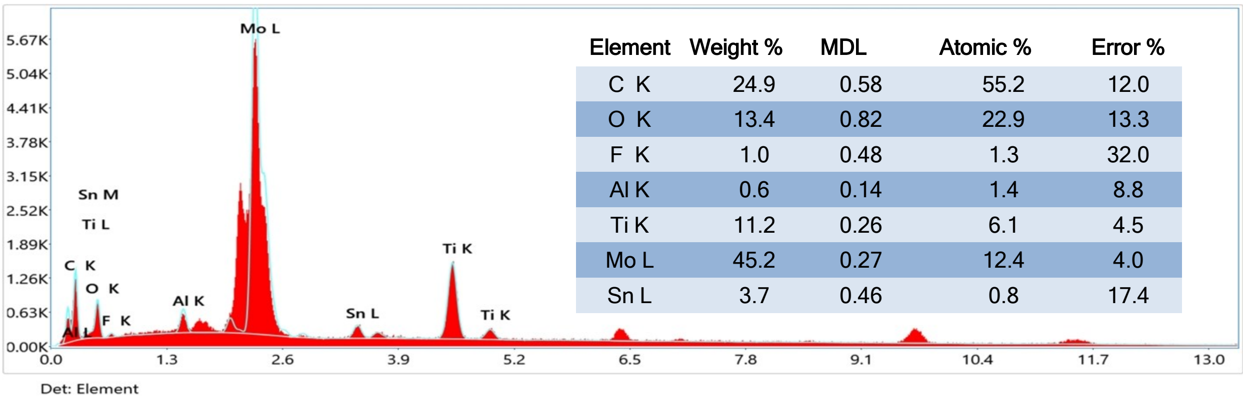

Element	Weight %	MDL	Atomic %	Error %
C K	24.9	0.58	55.2	12.0
O K	13.4	0.82	22.9	13.3
F K	1.0	0.48	1.3	32.0
Al K	0.6	0.14	1.4	8.8
Ti K	11.2	0.26	6.1	4.5
Mo L	45.2	0.27	12.4	4.0
Sn L	3.7	0.46	0.8	17.4

Figure 2: Sn@Mo2TiC2 MXene SEM image along with their EDX data.

The dependence of peak value current on scan rate was explained by using the following eq. SI1

$$I_p = a.v^b \tag{SI1}$$

Here a, b are constants, I_p represents the peak current and v used for scan rate, Generally the value of b=1 (capacitive process) b=0.5 (diffusion control dominated process) but most of the time in case of hybrid energy storage systems the value of b parameter lies between 1 and 0.5, which is evident of combine charge storage mechanism.

The formula used to measure the value of capacitance is written in eq. SI2 [1,2]

$$C = \frac{\int I(V)dV}{mv\Delta V} \tag{SI2}$$

Here C stands for specific capacitance (F g^{-1}), I(V)dV represents the integrated area of CV curve, m used to measure the mass of the active material (g), v stands the scan rate (mV s^{-1}) and ΔV represents the voltage window (V).

The eq. SI1 can be interpreted in this way by taking log on both sides.

$$\mathrm{Log}\ (I_p) = \mathrm{Log}\ (a) + b\log\ (v) \tag{SI3}$$

To study the combine charge storage mechanism further due capacitive process and diffusion control, we used the eq. SI4. Here the total peak current I_p is divided into k_1v (capacitive process) and $k_2v^{0.5}$ (diffusion control process) and represents the contribution of charge storage mechanism in both the ways.

$$I_p = k_1v + k_2v^{0.5} \tag{SI4}$$

After dividing with $v^{0.5}$ on both sides of eq. SI4, hence the obtained eq. SI5 basically provides the mathematical base to calculate the values of k_1 & k_2, which was further utilized to calculate the percentage contributions of diffusion control and capacitive process mechanism.

$$\frac{I_p}{v^{0.5}} = k_1 v^{0.5} + k_2 \quad \text{(SI5)}$$

Furthermore, the values of k_1 and k_2 can be determined by plotting a graph between $I/v^{0.5}$ and $v^{0.5}$ [3]. The slop represents the k_1 value and the point of intercept defines the value of k_2.

Table 1: Comparison of the current study with earlier published data.

Material	Electrolyte	Specific Capacitance (F/g)	References
Ti3C2Tx/PPy nanoparticles 2	1M Na2SO4	184	7
d-Ti3C2 (delaminated layers of Ti3C2)	H2SO4	320	8
Orthorhombic niobium pentoxide (T–Nb2O5)	H2SO4	330	9
Ti3C2Tx/PPy	1M H2SO4	416	10
Ti3C2Tx Aerogels	3M H2SO4	438	11
Nb-doped MXene (Ti3C2)	6M KOH	442	12
Ti3C2Tx/Ag2CrO4	0.1M H2SO4	525	13
Ni-doped Nb2C MXene	1M PVA–H2SO4	666	14
Sn@Mo2TiC2 MXene	1M KOH	670	This work

the eq. (SI6) shows the relationship between real impedance Z_{real} and angular frequency (ω) in low frequency region [4-6].

$$Z_{real} = R_s + R_{ct} + \sigma\, \omega^{-0.5} \quad \text{(SI6)}$$

Here σ belong to Warburg factor, which is calculated directly from the slop of the figure 7b. the coefficient of diffusion for K^+ ions can be calculated through following eq.SI7

$$D = \frac{R^2 T^2}{2A^2 n^4 F^4 C^2 \sigma^2} \quad \text{(SI7)}$$

Eq. SI7 clarifies the diffusion coefficient is directly proportional to R (gas constant) & T (absolute temperature) and inversely proportional to the A (surface area), n (no. of electrons), F (faraday constant), C (solution concentration) and D (diffusion coefficient).

References

1. A. Zaheer, S. A. Zahra, M. Z. Iqbal, A. Mahmood, S. A. Khan, S. Rizwan, Nickel-adsorbed two-dimensional Nb2C MXene for enhanced energy storage applications, *RSC Adv*., 2022, **12**, 4624.
2. S. A. Zahra, B. Anasori, M. Z. Iqbal, F. Ravaux, A. Tarawneh, Mohammednoor S. Rizwana, Enhanced electrochemical performance of vanadium carbide MXene composites for supercapacitors, *APL Materials*, 2022, **10**, 060901.
3. R. Li, X. Yu, X. Bian, F. Hu, Preparation, and electrochemical performance of VO_2 hollow spheres as a cathode for aqueous zinc ion batteries, *RSC Adv*., 2019, **9**, 35117.
4. H. Liu, et al. Kinetic study on $LiFePO_4$/C nanocomposites synthesized by solid state technique, *J. Power Sources*, 2006, **159**, 717–720.
5. A. J. Bard, L. R. Faulkner, Electrochemical Methods, *2 edn*, 2001, 211. (JOHN WILEY & SONS, INC. 2001)
6. S. Khamsanga1, R. Pornprasertsuk, T. Yonezawa, A. A. Mohamad, S. Kheawhom, δ-MnO_2 nanofower/graphite cathode for rechargeable aqueous zinc ion batteries, *Scientific Reports*, 2019, **9**, 8441.
7. A. Zaheer, S. A. Zahra, M. Z. Iqbal, A. Mahmood, S. A. Khan, S. Rizwan, Nickel-adsorbed two-dimensional Nb2C MXene for enhanced energy storage applications, *RSC Adv*., 2022, **12**, 4624.

8. T. Yaqoob, M. Rani, A. Mahmood, R. Shafique, S. Khan, N. K. Janjua, A. A. Shah, A. Ahmad, A. Abdullah, Al-Kahtani, MXene/Ag_2CrO_4 Nanocomposite as Supercapacitors Electrode, *Materials*, 2021, **14**, 6008.
9. X. Zang, J. Wang, Y. Qin, T. Wang, C. He, Q. Shao, H. Zhu, N. Cao, Enhancing capacitance performance of $Ti_3C_2T_x$ MXene as electrode materials of supercapacitor: From controlled preparation to composite structure construction, *Nano-Micro Lett.*, 2020, **12**, 77.

10. Y. Dall'Agnese, M. R. Lukatskaya, K. M. Cook, P. L. Taberna, Y. Gogotsi and P. Simon, High capacitance of surface modified 2D titanium carbide in acidic electrolyte, *Electrochem. Commun.,* 2014, **48**, 118–122,

11. C. Zhang, et al., Synthesis and charge storage properties of hierarchical niobium pentoxide/carbon/niobium carbide (MXene) hybrid materials, *Chem. Mater*., 2016, **28**(11), 3937–3943.

12. M. Boota, B. Anasori, C. Voigt, M. Q. Zhao, M. W. Barsoum, Y. Gogotsi, Pseudocapacitive electrodes produced by oxidant-free polymerization of pyrrole between the layers of 2D titanium carbide (MXene), *Adv. Mater*., 2016, **28**, 1517–1522.

13. X. Wang, Q. Fu, J. Wen, X. Ma, C. Zhu, X. Zhang, D. Qi, 3D Ti_3C_2Txaerogels with enhanced surface area for high performance supercapacitors, *Nanoscale* 2018, **10**, 20828–20835.

14. M. Fatima, et al., Nb-doped MXene with enhanced energy storage capacity and stability, front, Chem., 2020, **8**, 1–8.